

Engineering vascularized skeletal muscle tissue

Shulamit Levenberg^{1,2}, Jeroen Rouwkema³, Mara Macdonald², Evan S Garfein⁴, Daniel S Kohane⁵, Diane C Darland⁶, Robert Marini⁷, Clemens A van Blitterswijk³, Richard C Mulligan⁸, Patricia A D'Amore⁶ & Robert Langer²

One of the major obstacles in engineering thick, complex tissues such as muscle is the need to vascularize the tissue *in vitro*. Vascularization *in vitro* could maintain cell viability during tissue growth, induce structural organization and promote vascularization upon implantation. Here we describe the induction of endothelial vessel networks in engineered skeletal muscle tissue constructs using a three-dimensional multiculture system consisting of myoblasts, embryonic fibroblasts and endothelial cells cocultured on highly porous, biodegradable polymer scaffolds. Analysis of the conditions for induction and stabilization of the vessels *in vitro* showed that addition of embryonic fibroblasts increased the levels of vascular endothelial growth factor expression in the construct and promoted formation and stabilization of the endothelial vessels. We studied the survival and vascularization of the engineered muscle implants *in vivo* in three different models. Prevascularization improved the vascularization, blood perfusion and survival of the muscle tissue constructs after transplantation.

Most approaches to engineering new tissue have relied on the host for vascularization. Although this approach has been useful in many tissues, it has not been as successful in thick, highly vascularized tissues such as muscle^{1–3}. Skeletal muscle consists of individual muscle fibers arranged in parallel. Each fiber is a long, cylindrical multinucleated cell that is surrounded by connective tissue. Skeletal muscles have an abundant blood vessel supply, with branches of blood vessels following the connective tissue components of the muscle^{4,5}. So far, attempts to engineer skeletal muscle tissue have involved cultivation of skeletal myoblasts only, in some cases using growth factor delivery matrices or genetically engineered myoblasts to provide vascularization factors^{6–8}.

We hypothesized that embryonic endothelial cells in the appropriate environment could be used to induce endothelial vessel networks in engineered skeletal muscle tissue *in vitro*. First we developed a three-dimensional (3D) coculture system in which mouse myoblasts were mixed with human embryonic endothelial cells (hES cell-derived endothelial cells)⁹ or with human umbilical vein endothelial cells

(HUVECs) and seeded on highly porous, 3D biodegradable polymer scaffolds. The sponge-like scaffolds were composed of 50% poly(L-lactic acid) (PLLA) and 50% polylactic-glycolic acid (PLGA), with pore sizes of 225–500 μm^{10} (Fig. 1a).

As indicated by desmin immunostaining of cross sections of constructs 3 d after seeding of myoblasts, the myoblasts attached to and grew on the scaffolds (Fig. 1b). By 14 d the myoblasts had differentiated and formed partially aligned, elongated and multinucleated myotubes. Some of the myotubes differentiated further and became myogenin positive (36% \pm 3% of total nuclei) (Fig. 1b). When both myoblasts and endothelial cells (either hES cell-derived or HUVECs) were cultured on the scaffolds, the endothelial cells (CD31 positive) organized into tubular structures in between the myoblasts and throughout the construct, forming vessel networks within the engineered muscle tissue *in vitro* (Fig. 1c).

We compared the effects of two media: myoblast medium composed of DMEM with 10% FCS and 10% CS with HEPES and endothelial medium (EGM-2) with 2% FCS and endothelial growth factor supplements. Myoblast medium promoted both differentiation of the muscle cells (27% \pm 6% myogenin-positive nuclei) and formation of endothelial lumens in the constructs (Fig. 2a), whereas endothelial medium alone did not support differentiation of the muscle cells (2% \pm 1% myogenin-positive nuclei) and inhibited endothelial lumen formation (Fig. 2a). Why the endothelial medium inhibited vessel formation in the muscle constructs is not clear, and may be related to its inhibitory effect on muscle differentiation and cell signaling in the culture.

Because blood vessels are stabilized by association with pericytes or smooth muscle cells^{11–17} and because endothelial cells can induce the differentiation of undifferentiated mesenchymal cells into smooth muscle cells^{18–21}, we hypothesized that the formation of vessels characterized by lumen structures in the engineered skeletal muscle tissue would be promoted by embryonic fibroblasts. Addition of embryonic fibroblasts to the cultures, together with myoblasts and endothelial cells, strongly promoted vascularization of the engineered muscle; this was evidenced by increases in the total area of endothelial cells and the number and size of endothelial lumens, compared with constructs

¹Department of Biomedical Engineering, Technion 32000, Haifa, Israel. ²Department of Chemical Engineering, ³Division of Comparative Medicine, Massachusetts Institute of Technology, 77 Massachusetts Avenue, Cambridge, Massachusetts 02139, USA. ⁴Institute for Biomedical Technology, Twente University, Prof. Bronkhorstlaan 10-D, Bilthoven, 3723MB, The Netherlands. ⁵Department of Surgery, Brigham and Women's Hospital, 75 Francis St., 02115. ⁶Department of Pediatrics, Massachusetts General Hospital, 55 Fruit St., 02114. ⁷The Schepens Eye Research Institute and Department of Ophthalmology 20 Staniford St., 02114. ⁸Department of Molecular Medicine, Children's Hospital 300 Longwood Avenue, 02115, Harvard Medical School, Boston, Massachusetts, USA. Correspondence should be addressed to R.L. (rlanger@mit.edu) or S.L. (shulamit@bm.technion.ac.il).

seeded with myoblasts and endothelial cells only (Fig. 2a). The effect of the fibroblasts was dependent on medium conditions and the cell ratios (Fig. 2a, tri-cultures) with best vascularization in myoblast medium and addition of 0.2 million fibroblasts per scaffold (1.5 million cells total with 40–50% endothelial cells). The inductive effect of embryonic fibroblasts on endothelial vessels is shown even when comparing tri-culture samples that were seeded with a lower percentage (33%) of endothelial cells with cocultures of myoblasts and endothelial cells seeded with higher percentages of endothelial cells (40–50%) (Fig. 2a).

To analyze the stability of the *in vitro* vessel-like structures formed in the muscle constructs, we examined tri-culture constructs (a combination of myoblasts, fibroblasts and endothelial cells) at 2 weeks and 1 month. Large vessel structures ($>1,500 \mu\text{m}^2$) were evident only in the 1-month-old tri-culture constructs (Fig. 1c). In addition, tri-cultures grown for 1 month had a twofold increase in the number of endothelial structures, a greater surface area covered by endothelial cells and a higher percentage of vessel-like structures with lumens, compared with 2-week tri-cultures (Fig. 2b).

These results suggest that addition of embryonic fibroblasts promoted stabilization of the vessel structures over time. Double labeling for von Willebrand factor (vWF) and smooth muscle actin on cross sections of constructs seeded with endothelial cells and embryonic fibroblasts showed that fibroblasts in the cultures became smooth-muscle-actin positive (suggesting differentiation into smooth muscle cells) and were colocalized around endothelial cells in vessel-like structures (Fig. 2c). Quantitative analysis of the double staining revealed that $65.7\% \pm 8.8\%$ of endothelial vessel-like structures in the constructs had associated smooth muscle cells.

To study the expression of key vasculogenic and angiogenic factors in the 3D muscle constructs, we analyzed the expression of vascular endothelial growth factor (VEGF) and platelet-derived growth factor (PDGF)-B at the mRNA level in the muscle constructs. The RT-PCR results showed that addition of human endothelial cells to myoblast or fibroblast cultures resulted in an increase in mouse VEGF expression. Moreover, tri-cultures that included embryonic fibroblasts had higher levels of VEGF mRNA than myoblast-endothelial cocultures (Supplementary Fig. 1 online). The increased VEGF expression is consistent with the increase in the endothelial network observed in the tri-cultures, and could be one of the factors affecting the induction of vascularization of the constructs. Indeed, addition of VEGF to the medium resulted in a larger area covered by endothelial cells and an increase in the number of vessel-like endothelial tubular structures in the constructs (Fig. 2d). Depletion of VEGF from the medium resulted in a decreased number of vessel structures, whereas addition

of fibroblasts to cultures without VEGF supplementation restored vessel formation (data not shown).

To assess the therapeutic potential of our approach, we used three models to analyze the survival, differentiation, integration and vascularization of the implant *in vivo*: (i) subcutaneous implantation in the back of severe combined immunodeficient (SCID) mice, (ii) intramuscular implantation into the quadriceps muscle of nude rats, and (iii) replacement of the anterior abdominal muscle segment of nude mice with the construct. In all three models the muscle implant continued to differentiate *in vivo*. The implanted myotubes were elongated and multinucleated (6–8 nuclei), with a high percentage of myogenin-positive myotubes ($67\% \pm 9\%$) (Fig. 3a). Control implants containing fibroblasts or no cells showed no desmin-positive myotubes or myogenin-positive nuclei within the scaffold area (Fig. 3a). To further ensure that the myotubes observed within the scaffold were derived from implanted cells rather than invading host

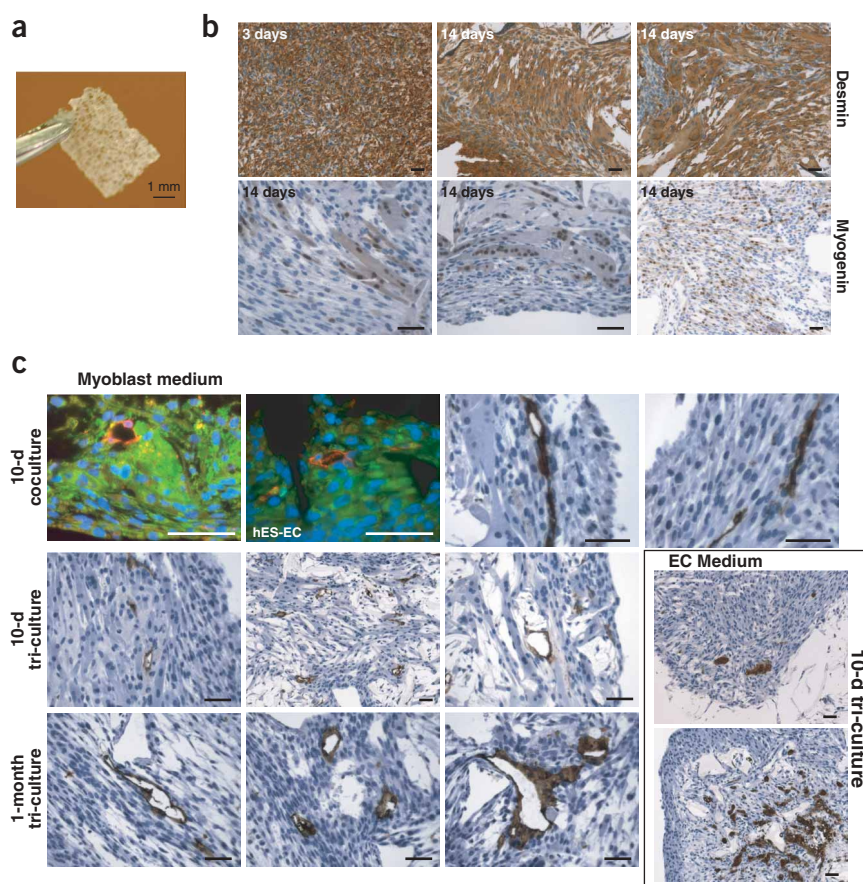


Figure 1 *In vitro* vascularization of engineered skeletal muscle tissue (a) PLLA/PLGA scaffold before cell seeding. Scale bar, 1 mm. (b) Myocyte differentiation on PLLA/PLGA polymer scaffolds. Desmin and myogenin immunostaining of tissue sections taken from 3D scaffolds cocultured with skeletal myoblasts and endothelial cells (HUVEC) and grown for 3 d and 14 d. Scale bar = 50 μm . (c) Vessel-like network formation *in vitro* in muscle 3D constructs. Endothelial cells (HUVEC or hES cell-derived endothelial cells (hES-EC) when indicated) were coseeded with skeletal myoblasts on polymer scaffolds and grown for 10 d (cocultures). Tissue construct sections were immunofluorescently stained using anti-CD31 antibodies (red), anti-desmin antibodies (green) and DAPI for nuclear staining (blue) (left), or stained using anti-CD31 antibodies alone (brown) and counterstained with hematoxylin (blue) (right). One-month tri-cultures and 10-d, both including mouse embryonic fibroblasts, were grown either in myoblast medium or endothelial medium (EC medium) and stained using anti-CD31 antibodies. Cultured cell numbers (myoblast/endothelial/fibroblast), $0.5/0.7/0.2 \times 10^6$; bottom picture in endothelial (EC) medium, $0.5/0.5/0.5 \times 10^6$. Scale bar, 50 μm .

cells, we incorporated 5-bromodeoxyuridine (BrdU) in the tissue-engineered constructs before implantation. BrdU labeling confirmed that the implanted myoblasts had indeed survived and differentiated to populate the scaffold (data not shown). In most cases, particularly in the abdominal muscle, the implanted myotubes were in close contact with the host muscle, with very thin and sometimes barely detectable fibrous tissue around the implant (Fig. 3a). The myotubes in the implanted area were relatively long and thick and in many cases appeared to have reoriented themselves to align with the fibers of the host tissue (Fig. 3a).

The constructs were permeated with host blood vessels (Fig. 3b). Quantification of the number of endothelial vessel-like structures in intramuscular implants 2 weeks after implantation indicated that there

was no significant difference between constructs seeded with HUVECs or hES cell-derived endothelial cells (Supplementary Fig. 2 online). Staining of subcutaneous implants with anti-human specific endothelial antibodies (anti-CD31) demonstrated the presence of vessels (between elongated myotubes), which were lined by implanted human endothelial cells. Moreover, construct-derived vessels contained intraluminal red blood cells, suggesting that vessels had anastomosed with the host vasculature (Fig. 3b).

To determine whether the vessels were functional, we injected labeled lectin into the tail vein 2 weeks after implantation and counted the perfused vessels. The results indicated that $41\% \pm 12\%$ of human CD31-positive vessels (implant-derived vessels) were perfused with lectin. Quantification of the total number of

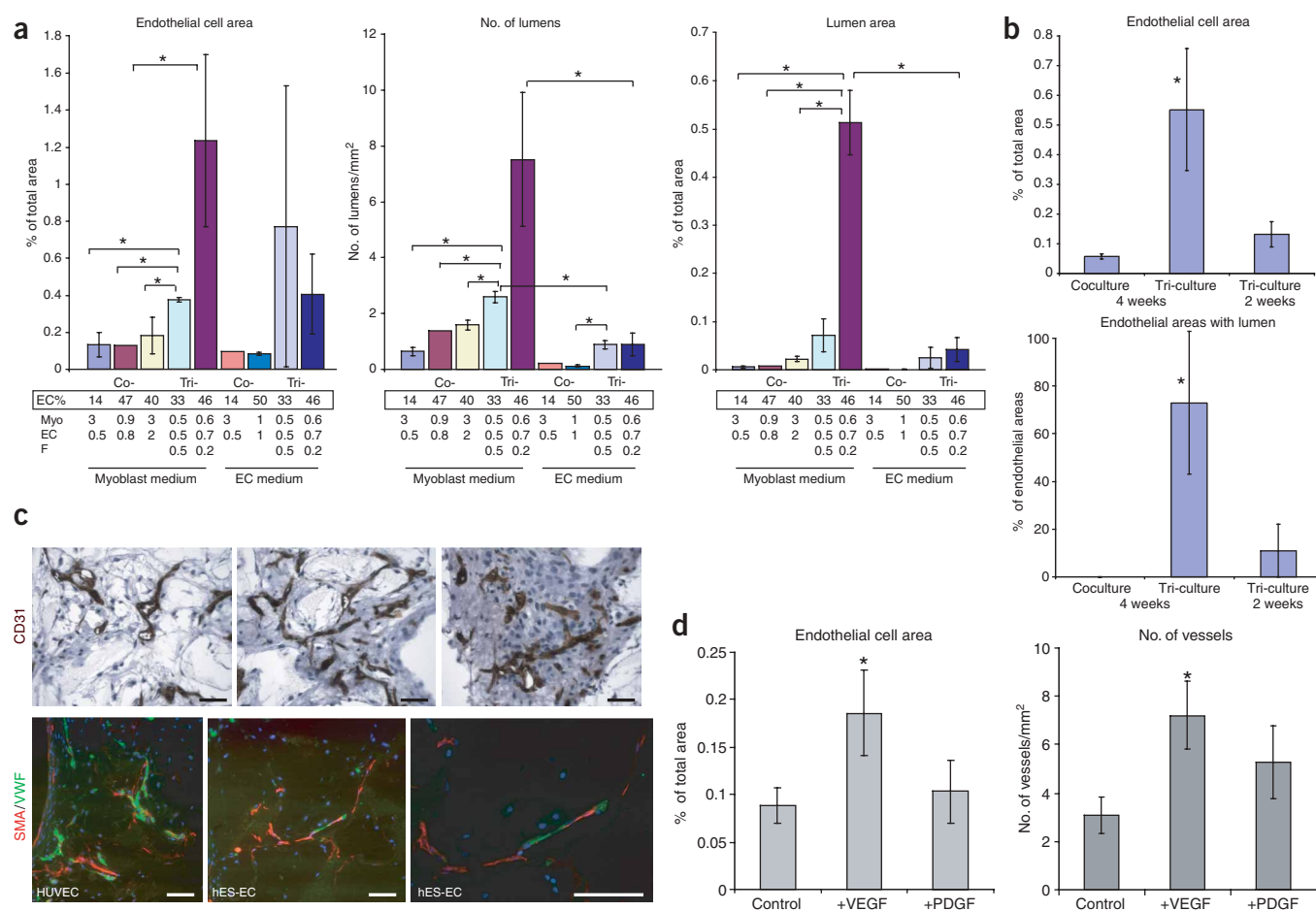


Figure 2 Quantitative analysis of endothelial vessels in muscle constructs, *in vitro*. (a) Comparison of vessel formation in coculture (Co) and tri-culture (Tri) constructs grown with different cell ratios (cell number $\times 10^6$) and medium conditions (myoblast medium and endothelial medium). Endothelial cell ratio (EC %) is calculated as percentage of the total cell number. Endothelial cell area corresponds to percentages of area positively stained with CD31 antibody within the tissue section. Lumen area shows the total area of all the lumens in the section as percentages of total section area. Myo, myoblasts; EC, endothelial cells (HUVEC); F, mouse embryonic fibroblasts. * denotes statistical significance ($P < 0.05$) between the indicated pairs. (b) Comparison of vessels in 2-week and 4-week constructs. Cocultures are myoblasts and endothelial cells (0.8 and 0.6×10^6 cells per scaffold, respectively). Tri-cultures are myoblasts, fibroblasts and endothelial cells (0.6 , 0.2 and 0.6×10^6 cells per scaffold respectively). * denotes statistical significance ($P < 0.05$) compared with controls. (c) Effect of embryonic fibroblasts on vessel formation. Constructs seeded with embryonic fibroblasts and endothelial cells ($0.5, 1 \times 10^6$) were grown for 2 weeks. Construct sections were immunostained with human-specific anti-CD31 antibodies (brown) showing vessel formation throughout the 3D constructs. Colocalization of smooth muscle cells and endothelial cells (HUVEC or hES-EC as indicated). Constructs were immunofluorescently double-stained using anti-VWF antibodies (green), anti-smooth muscle actin antibodies (red) and DAPI for nuclear localization. Note smooth muscle actin-positive cells around elongated endothelial structures. Scale bar, $50 \mu\text{m}$. (d) Effect of VEGF or PDGF-B supplementation on endothelial vessel formation. Tri-culture constructs (myoblasts, fibroblasts and endothelial cells (0.6 , 0.2 and 0.7×10^6 cells per scaffold, respectively)) were incubated with control medium or medium supplemented with VEGF (50 ng/ml) or PDGF-B (5 ng/ml). After 2 weeks, construct sections were immunoassayed using anti-CD31 antibodies and analyzed for endothelial-positive area, and number of endothelial vessels. * denotes statistical significance ($P < 0.05$) compared with controls. The results shown are mean values \pm s.d. ($n = 4$).

perfused vessels (host and implant derived) indicated that muscle constructs seeded with endothelial cells had 30 ± 2 functional vessels per square millimeter compared with 21 ± 2 vessels in constructs seeded with muscle cells only ($n = 3$, $P < 0.01$). The size distribution of functional vessels showed that including endothelial cells in the scaffolds also increased the number of larger or stabilized vessels in the muscle implants (Fig. 3c). These results suggest that pre-endothelialization of the construct, by promoting implant vascularization, can improve blood perfusion to the muscle implant and implant survival *in vivo*.

To further evaluate tissue-engineered muscle construct survival and integration *in vivo*, we used a luciferase-based imaging system.

The *in vivo* imaging system (IVIS) works by detecting light generated by the interaction of systemically administered luciferin with locally produced luciferase. Muscle constructs seeded with or without endothelial cells or fibroblasts, and control constructs were infected with adeno-associated virus (AAV) vector, encoding luciferase, for 48 h before transplantation. Detection of luciferase expression in the constructs indicated no difference among the various muscle constructs *in vitro*. The constructs were then placed *in situ* in the anterior abdominal muscle walls of nude mice. Three weeks after surgery, the mice received luciferin (injected subcutaneously on the dorsal surface) to assess perfusion to the tissue-engineered construct. A minimal signal was detected in areas that did not receive gene transfer or

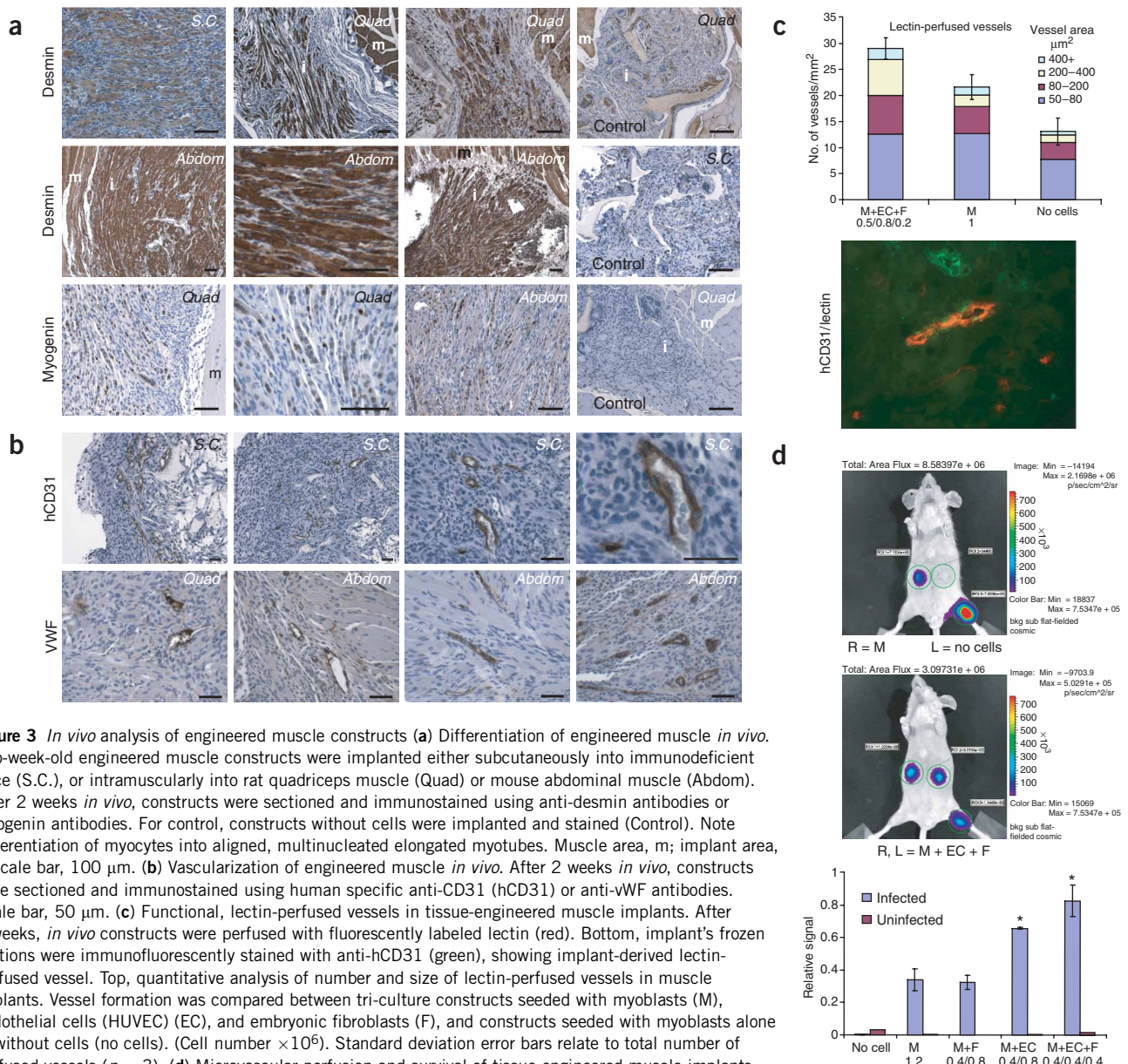


Figure 3 *In vivo* analysis of engineered muscle constructs (a) Differentiation of engineered muscle *in vivo*. Two-week-old engineered muscle constructs were implanted either subcutaneously into immunodeficient mice (S.C.), or intramuscularly into rat quadriceps muscle (Quad) or mouse abdominal muscle (Abdom). After 2 weeks *in vivo*, constructs were sectioned and immunostained using anti-desmin antibodies or myogenin antibodies. For control, constructs without cells were implanted and stained (Control). Note differentiation of myocytes into aligned, multinucleated elongated myotubes. Muscle area, m; implant area, i. Scale bar, 100 μm . (b) Vascularization of engineered muscle *in vivo*. After 2 weeks *in vivo*, constructs were sectioned and immunostained using human specific anti-CD31 (hCD31) or anti-vWF antibodies. Scale bar, 50 μm . (c) Functional, lectin-perfused vessels in tissue-engineered muscle implants. After 2 weeks, *in vivo* constructs were perfused with fluorescently labeled lectin (red). Bottom, implant's frozen sections were immunofluorescently stained with anti-hCD31 (green), showing implant-derived lectin-perfused vessel. Top, quantitative analysis of number and size of lectin-perfused vessels in muscle implants. Vessel formation was compared between tri-culture constructs seeded with myoblasts (M), endothelial cells (HUVEC) (EC), and embryonic fibroblasts (F), and constructs seeded with myoblasts alone or without cells (no cells). (Cell number $\times 10^6$). Standard deviation error bars relate to total number of perfused vessels ($n = 3$). (d) Microvascular perfusion and survival of tissue-engineered muscle implants. Cells in the constructs were infected with AAV-luciferase for 48 h before transplantation. Control constructs were not infected with virus. The constructs were then placed *in situ* in the anterior abdominal muscle walls of nude mice. AAV-luciferase was injected into the left lower extremity of each mouse at the time of surgery to serve as a positive control. Three weeks after surgery, the mice received luciferin to assess perfusion and survival of the tissue engineered implants using luciferase-based *in vivo* imaging system (IVIS). Quantification of signal detected after 3 weeks. The results are mean values \pm s.d. ($n = 3$). * denotes statistical significance ($P < 0.05$) compared with myoblasts alone (M) or myoblasts + fibroblasts (M+F). (Cell number $\times 10^6$). Signal intensities are shown on a scale of purple to red ($\sim 2 \times 10^4$ to $\sim 7.7 \times 10^5$ p/s/cm²).

in constructs that were not seeded with cells. However strong signals were detected from areas either directly transduced with AAV-luciferase (as controls) or transplanted with virally transduced cells, indicating perfused vessels. By using the luciferase system, we were able to noninvasively determine the degree to which different constructs continued to survive (and express luciferase) and maintain vascular connections with the recipient to receive systemically delivered luciferin. The relative signal detected in implants seeded with endothelial cells in cocultures (with myoblasts) and in tri-cultures (with myoblasts and fibroblasts) was higher than in myoblast-only implants (Fig. 3d). Coupled with similar preimplantation levels of luciferase expression and with the histological evidence of increased functional vascularity, the results suggest that the increased signal in pre-endothelialized samples is related to increased perfusion and survival of the tissue-engineered muscle constructs. Analysis of cell survival in the implant using TUNEL staining indicated a twofold increase in the number of apoptotic cells in muscle-only implants compared with pre-endothelialized implants (36 ± 9 and 19 ± 7 cells per implant, respectively ($n = 3$)).

The approach that we have developed enables formation and stabilization of endothelial vessel networks *in vitro* in 3D engineered skeletal muscle tissue. The overall *in vivo* results show that prevascularization of the implants improves implant vascularization and survival. Unlike previous studies demonstrating endothelial differentiation within fibroblast culture and fibroblast differentiation into pericytes^{11,14,15}, this study demonstrates engineering of 3D vascularized skeletal muscle constructs with formation of endothelial networks throughout and in between differentiating skeletal muscle fibers. This study emphasizes the importance of multicell cultures in providing appropriate signals for vascular organization in skeletal muscle tissue. Moreover, it provides evidence for the potential of endothelial cocultures in promoting *in vivo* vascularization of engineered tissues. Cocultures with endothelial cells may also be important for inducing differentiation of engineered tissues, as embryonic endothelial cells are critical for the earliest stages of organogenesis^{22,23}. We believe that this approach could have potential applications in tissue engineering and may provide a tool for the *in vitro* study of multicellular processes such as tissue vascularization.

METHODS

Cell culture. Mouse skeletal myoblast cells (C_2C_{12})^{24,25} were cultured in DMEM supplemented with 10% FBS, 10% calf serum and 2.5% HEPES buffer. Human umbilical vein endothelial cells (HUVEC) were cultured in endothelial cell medium (EGM-2; Cambrex Biosciences). Mouse embryonic fibroblasts (MEF) (Cell Essentials) were cultured in DMEM supplemented with 10% FBS. HES cell-derived CD31+ endothelial cells were isolated as described⁹ and cultured in endothelial cell medium.

Polymer scaffolds. Porous sponges composed of 50% PLLA and 50% PLGA were fabricated as described¹⁰ with pore sizes of 225–500 μm and 93% porosity. The PLGA was selected to degrade quickly (~ 3 weeks) to facilitate cellular ingrowth, whereas the PLLA was chosen to provide mechanical support to 3D structures. The degradation time of the composed sponges is ~ 6 months. Biocompatibility of PLLA and PLGA porous scaffolds was previously shown²⁶. For seeding, the desired number of cells were pooled and resuspended in 7–15 μl of a 1:1 mixture of culture medium and growth factor-reduced Matrigel (BD Biosciences). This suspension was allowed to absorb into the sponges, after which the sponges were incubated for 30 min at 37 °C to allow solidification of the gel. Culture medium was then added, the sponges were detached from the bottom, and incubated at 37 °C on a XYZ shaker. The medium was changed every other day. At the conclusion of the experiments, samples were fixed in 10% formalin and subsequently embedded in paraffin for sectioning or were transplanted into mice or rats.

Implantation of muscle constructs. Male 5- to 6-week-old SCID mice (CB.17 SCID) were anesthetized with 2.5% isoflurane in balanced oxygen, after which a construct was implanted subcutaneously on each side lateral to the dorsal midline region of each mouse. For intramuscular implantation, constructs were implanted into the outer quadriceps muscle of the right-hand side of 5- to 7-week-old male nude rats. Sutures of 6-0 Prolene in a simple interrupted pattern were used to prevent movement of the constructs from the muscle site, and the skin was closed using surgical staples. Two to eight weeks after implantation, the mice or rats were killed and the implants were retrieved. Samples were fixed in 10% natural buffered formalin, processed routinely and sectioned at 4 μm before staining. Two assays were involved in perfusion analysis. (i) Lectin perfusion. Lectin HPA (*Helix pomatia* agglutinin) conjugated to Alexa Fluor 594 (Molecular Probes) (0.5 mg/0.25 ml PBS) was injected into the tail vein of anesthetized animals (20 mg/kg body weight). Circulation was allowed for 2 min after which the animals were killed and the implants were retrieved. Samples were snap frozen (liquid nitrogen) in Cryomatrix (Thermo Shandon) and sections of 6 μm were cut with a cryotome. (ii) Luciferase assay (abdominal wall model). Tissue-engineered constructs were placed in 12-well culture dishes in 2 ml of medium and 1.0×10^9 dot blot/cc of AAV-luciferase added. After 48 h, the constructs were washed with two volumes of PBS. As a control, luciferin (150 μl of 5mg/ml) was added to each well. After incubation for 11 min, the constructs were imaged in the Xenogen IVIS device at a 3-minute exposure. Luminescence was determined by calculating the flux (photons/sec/cm²) overlying each construct. Immediately thereafter, the constructs were implanted into isoflurane-anesthetized mice by creation of a 3 mm \times 3 mm defect in the anterior abdominal wall of the mice in line with the inferior epigastric artery. The construct was then sutured in place using four 7-0 prolene sutures attached to each corner of the construct. After the ventral skin was sutured, the animal recovered. At various intervals after surgery, the animals were imaged using the Xenogen IVIS device. Mice were anesthetized using an intramuscular injection of ketamine and xylazine. Luciferin (150 μl of 5 mg/ml) was injected subcutaneously on the dorsal surface of the mouse and allowed to circulate for 11 min before the animals were imaged. Luminescence was calculated by determining the photon flux. A 1.0 cm² area was chosen arbitrarily as the standard. The ratio of the flux from the tissue-engineered construct relative to the hind limb was calculated. After the final imaging session, the animals were killed and the implants were retrieved and placed in 10% formalin before routine processing and histological sectioning. Unseeded scaffolds were used as controls and showed host-cell infiltration (including fibroblasts and blood vessels) as known from previous studies²⁶.

Tissue processing and immunohistochemical staining. Tissue constructs were fixed for 6 h in 10% neutral buffered formalin, routinely processed, and embedded in paraffin. Transverse sections (4 μm) were placed on silanized slides for immunohistochemistry or staining with hematoxylin and eosin. Immunohistochemical staining was carried out using the Biocare Medical Universal HRP-DAB kit (Biocare Medical) according to the manufacturer's instructions, with prior heat treatment at 95 °C for 20 min in ReVeal buffer (Biocare Medical) for epitope recovery. For immunofluorescent staining, the secondary antibodies used were Alexa Fluor (Molecular Probes) and Cy-3 (Jackson Laboratories) followed by DAPI (Sigma) nuclear staining. The primary antibodies were anti-human: CD31 (1:20); desmin (1:150); α -smooth muscle actin (1:50); vWF (1:200) (all from Dako); or vWF (Chemicon) (1:100). Staining with α -smooth muscle actin antibody (as well as other smooth muscle actin markers to identify fibroblasts differentiation into smooth muscle cells could not be done in the presence of C_2C_{12} cells because of expression of these markers by the C_2C_{12} myoblasts. The vWF antibody was used after deparaffinization and trypsin treatment for epitope recovery. For labeling implanted myoblasts, myoblast culture medium was supplemented with 10 μm of 5'-bromo-2'-deoxyuridine (BrdU) (Sigma) and applied to 60% confluent dish cultures for 16 h. Cells were washed and seeded on scaffolds as described. Tissue sections were stained using mouse anti-BrdU antibodies (1:1,000) as described, but with treatment with 2N HCL and 0.5% Triton X-100 for 30 min at 37 °C to denature the DNA, before addition of the antibodies. For staining apoptotic cells DeadEnd colorimetric TUNEL system (Promega) was used.

RT-PCR analysis. Total RNA was isolated by an RNEasy Mini Kit (Qiagen), using the isolation-from-tissue protocol. RT-PCR was carried out using a Qiagen OneStep RT-PCR kit with 10 units Rnase inhibitor (Gibco) and 40 ng RNA. To ensure semi quantitative results of the RT-PCR assays the number of PCR cycles for each set of primers was checked to be in the linear range of the amplification. Primer sequences: mouse VEGF, 5'-CCT CCG AAA CCA TGA ACT TTC TGC TC-3' and 5'-CAG CCT GGC TCA CCG CCT TGG CTT-3'; human PDGF-B, 5'-GGA GCA TTT GGA GTG CGC CT-3' and 5'-ACA TCC GTG TCC TGT TCC CGA-3'.

The amplified products were separated on 1.2% agarose gels with ethidium bromide (E-Gel, Invitrogen). Mean pixel intensities of each band were measured and normalized to mean pixel intensities of glyceraldehyde phosphodehydrogenase band. The values for two experiments (performed in duplicate) were then averaged and graphed with s.d.

Image analysis. Overlapping microscopic pictures were taken at a magnification of 100× so that the entire area of the sample was covered. An imaging software (AxioVision 3.1, Carl Zeiss) was used to determine the area of endothelial cells, the area of vessels or lumen and the total sample area. The number of structures with lumen was counted manually. For colocalization analysis, 3–6 randomly chosen 20× fields were analyzed using OpenLab (Density Slice Module) image analysis software (ImproVision) to quantify endothelial cell-positive areas with and without colocalization of smooth muscle cell-positive areas. An endothelial cell-positive area was identified by the presence of a vWF-positive vessel-like structure with a lumen. *P* values were calculated using Student's *t*-test.

Note: Supplementary information is available on the Nature Biotechnology website.

ACKNOWLEDGMENTS

The authors thank the MIT division of comparative medicine for excellent assistance in tissue embedding and processing, Adam Kapur for help with data analysis, and Justin S. Golub for help with RT-PCR assays. We would like to thank Joseph Itskovitz-Eldor for assistance and cooperation in conducting this research. This work was supported by National Institutes of Health grants HL60435 (R.L. and S.L.) and EY05318 (P.A.D. and D.C.D.).

COMPETING INTERESTS STATEMENT

The authors declare that they have no competing financial interests.

Received 26 January; accepted 2 May 2005

Published online at <http://www.nature.com/naturebiotechnology/>

1. Saxena, A.K., Marler, J., Benvenuto, M., Willital, G.H. & Vacanti, J.P. Skeletal muscle tissue engineering using isolated myoblasts on synthetic biodegradable polymers: preliminary studies. *Tissue Eng.* **5**, 525–532 (1999).
2. Neumann, T., Nicholson, B.S. & Sanders, J.E. Tissue engineering of perfused microvessels. *Microvasc. Res.* **66**, 59–67 (2003).

3. Bach, A.D., Stem-Straeter, J., Beier, J.P., Bannasch, H. & Stark, G.B. Engineering of muscle tissue. *Clin. Plast. Surg.* **30**, 589–599 (2003).
4. Wigmore, P.M. & Evans, D.J. Molecular and cellular mechanisms involved in the generation of fiber diversity during myogenesis. *Int. Rev. Cytol.* **216**, 175–232 (2002).
5. Buckingham, M. Skeletal muscle formation in vertebrates. *Curr. Opin. Genet. Dev.* **11**, 440–448 (2001).
6. Zisch, A.H., Lutolf, M.P. & Hubbell, J.A. Biopolymeric delivery matrices for angiogenic growth factors. *Cardiovasc. Pathol.* **12**, 295–310 (2003).
7. von Degenfeld, G., Banfi, A., Springer, M.L. & Blau, H.M. Myoblast-mediated gene transfer for therapeutic angiogenesis and arteriogenesis. *Br. J. Pharmacol.* **140**, 620–626 (2003).
8. Lu, Y. *et al.* Recombinant vascular endothelial growth factor secreted from tissue-engineered bioartificial muscles promotes localized angiogenesis. *Circulation* **104**, 594–599 (2001).
9. Levenberg, S., Golub, J.S., Amit, M., Itskovitz-Eldor, J. & Langer, R. Endothelial cells derived from human embryonic stem cells. *Proc. Natl. Acad. Sci. USA* **99**, 4391–4396 (2002).
10. Levenberg, S. *et al.* Differentiation of human embryonic stem cells on three-dimensional polymer scaffolds. *Proc. Natl. Acad. Sci. USA* **100**, 12741–12746 (2003).
11. Darland, D.C. & D'Amore, P.A. TGF beta is required for the formation of capillary-like structures in three-dimensional cocultures of 10T1/2 and endothelial cells. *Angiogenesis* **4**, 11–20 (2001).
12. Carmeliet, P. Angiogenesis in health and disease. *Nat. Med.* **9**, 653–660 (2003).
13. Jain, R.K. Molecular regulation of vessel maturation. *Nat. Med.* **9**, 685–693 (2003).
14. Sieminski, A.L., Padera, R.F., Blunk, T. & Gooch, K.J. Systemic Delivery of Human Growth Hormone Using Genetically Modified Tissue-Engineered Microvascular Networks: Prolonged Delivery and Endothelial Survival with Inclusion of Nonendothelial Cells. *Tissue Eng.* **8**, 1057–1069 (2002).
15. Koike, N. *et al.* Tissue engineering: creation of long-lasting blood vessels. *Nature* **428**, 138–139 (2004).
16. Black, A.F., Berthod, F., L'Heureux, N., Germain, L. & Auger, F.A. *In vitro* reconstruction of a human capillary-like network in a tissue-engineered skin equivalent. *FASEB J.* **12**, 1331–1340 (1998).
17. Shinoka, T. Tissue engineered heart valves: autologous cell seeding on biodegradable polymer scaffold. *Artif. Organs* **26**, 402–406 (2002).
18. Flamme, I., Frolich, T. & Risau, W. Molecular mechanisms of vasculogenesis and embryonic angiogenesis. *J. Cell. Physiol.* **173**, 206–210 (1997).
19. Rossant, J. & Hirashima, M. Vascular development and patterning: making the right choices. *Curr. Opin. Genet. Dev.* **13**, 408–412 (2003).
20. Hirschi, K.K., Rohovsky, S.A. & D'Amore, P.A. PDGF, TGF-beta, and heterotypic cell-cell interactions mediate endothelial cell-induced recruitment of 10T1/2 cells and their differentiation to a smooth muscle fate. *J. Cell Biol.* **141**, 805–814 (1998).
21. Darland, D.C. *et al.* Pericyte production of cell-associated VEGF is differentiation-dependent and is associated with endothelial survival. *Dev. Biol.* **264**, 275–288 (2003).
22. Lammert, E., Cleaver, O. & Melton, D. Induction of pancreatic differentiation by signals from blood vessels. *Science* **294**, 564–567 (2001).
23. Matsumoto, K., Yoshitomi, H., Rossant, J. & Zaret, K.S. Liver organogenesis promoted by endothelial cells prior to vascular function. *Science* **294**, 559–563 (2001).
24. Yaffe, D. & Saxel, O. Serial passaging and differentiation of myogenic cells isolated from dystrophic mouse muscle. *Nature* **270**, 725–727 (1977).
25. Blau, H.M. *et al.* Plasticity of the differentiated state. *Science* **230**, 758–766 (1985).
26. Holder, W.D. Jr. *et al.* Cellular ingrowth and thickness changes in poly-L-lactide and polyglycolide matrices implanted subcutaneously in the rat. *J. Biomed. Mater. Res.* **41**, 412–421 (1998).